

N88-14885

511-18

116674

208.

ANALYSIS AND INTERPRETATION OF SATELLITE FRAGMENTATION DATA

Final Report

AM 5/4835

NASA/ASEE Summer Faculty Fellowship Program - 1987

Johnson Space Center

Prepared by: Arjun Tan
Academic Rank: Associate Professor
University & Department: Alabama A&M University
Department of Physics
Normal, Alabama 35762

NASA/JSC

Directorate: Space and Life Sciences Directorate
Division: Solar System Exploration Division
Branch: Space Science Branch
JSC Colleague: Gautam D. Badhwar
Date: August 14, 1987
Contract Number: NGT 44-001-800

ABSTRACT

The velocity perturbations of the fragments of a satellite can shed valuable information regarding the nature and intensity of the fragmentation. A feasibility study on calculating the velocity perturbations from existing equations was carried out by analyzing 23 major documented fragmentation events. It was found that whereas the calculated values of the radial components of the velocity change were often unusually high, those in the two other orthogonal directions were mostly reasonable. Since the uncertainties in the radial component necessarily translate into uncertainties in the total velocity change, it is suggested that alternative expressions for the radial component of velocity be sought for the purpose of determining the cause of the fragmentation from the total velocity change. The calculated variances in the velocity perturbations in the two directions orthogonal to the radial vector indicate that they have the smallest values for collision induced breakups and the largest values for low-intensity explosion induced breakups. The corresponding variances for high-intensity explosion induced breakups generally have values intermediate between those of the two extreme categories. A three-dimensional plot of the variances in the two orthogonal velocity perturbations and the plane change angle shows a clear separation between the three major types of breakups. This information is used to reclassify a number of satellite fragmentation events of unknown category.

INTRODUCTION

Since the launch of Sputnik 1, over 16,000 pieces of man-made objects have circled the earth (NSSC Satellite Catalog, 1985). Of these, almost 6,000 are still in orbit, but only 5 percent are useful functioning satellites (Johnson, 1985). The number of smaller, untrackable and uncataloged objects is believed to be several times higher (Sehnal, 1984; Taff, et al., 1984).

Almost half of the cataloged orbital "debris" originated from the fragmentation of satellites. As of January 1986, over 90 documented cases of satellite fragmentation events have taken place (Johnson, et al., 1986). Each event can create up to several hundreds of additional trackable debris plus an unknown number of untrackable ones, thus increasing the population of unwanted, hazardous material in space.

Satellites can break up from explosions or through collisions with other objects. Of these, explosion has been the major cause of breakups. According to Bess (1975), two classes of explosions are recognized. In a high-intensity explosion, the explosive charge is in direct contact with the spacecraft structure, e.g., ignition of excess fuel. In a low-intensity explosion, on the other hand, the charge is not in direct contact with the spacecraft structure, e.g., a pressure vessel explosion.

Satellites can also break up from collision with a man-made object or a natural meteorite. A collision can be part of an anti-satellite testing. In low earth orbit space, the average relative velocity of collisions between two objects is calculated to be about 10 km/s (Kessler and Cour-Palais, 1978), thus placing the collision in the hypervelocity range. The average relative angle between two colliding objects is estimated to be around 90 degrees (Chobotov, 1983).

The cataloged satellite fragmentation events have been categorized into the following three classes (Johnson, et al., 1986). About one-sixth are

due to propulsion related causes -- valve failure in a rocket motor, mixing of volatile fuels, ignition of excess fuel, etc. About a third have been deliberate -- anti-satellite testing, destruction of sensitive hardware or malfunctioning equipment. The remaining half of all breakups are of unknown cause -- there was little or no fuel on board and no trackable objects nearby. This raises the serious concern about the possibility that some of the unknown breakup cases might have been due to collision with a small untrackable object.

An early effort in using debris characteristics as a tool to distinguish between explosion and collision induced satellite breakups was carried out by Culp and McKnight (Culp, 1986). They developed a Satellite Fragmentation Event (SAFE) Test, which generates a score as to the more probable cause of fragmentation: explosion or collision. The mass distribution of the fragments as inferred from radar cross-section measurements were compared with those of earth-based explosion and collision experiments from Bess (1975). Also considered in the SAFE Test were the relative dispersion of larger fragments, orderliness and symmetry of Gabbard diagrams and the dependence of velocity perturbations on mass.

The SAFE Test has been deemed fairly successful in distinguishing between explosions and small particle collisions but is somewhat subjective in nature as it depends upon the skill of the performer. Also, the Gabbard diagrams are altered by the "age" of the data due to atmospheric drag and the best data just after the event are generally unavailable.

One parameter that is least affected by the age of the data is the plane change angle of the fragments, since the inclination of a satellite is unaffected by atmospheric drag. Badhwar, et al. (1987) utilized this fact to develop a scheme of determining the cause of satellite fragmentation which is both objective and free from the "ageing" effect of the data. Based on the distribution characteristics of the plane

change angles and radar cross-sections of known fragmentation cases, they came up with a scheme to distinguish between three classes of satellite breakups: collision induced, high-intensity explosion induced and low-intensity explosion induced breakups.

A set of quantities which can be readily calculated from the fragment data using existing equations and which can provide valuable information regarding the breakup are the velocity changes imparted to the fragments during the fragmentation event. McKnight (Culp, 1986) and Kling (1986) pursued this course to some extent, but lately, such efforts have been quietly abandoned because the results obtained were often thought to be unrealistic (Reynolds, 1987).

In the present study, we have re-examined the feasibility of the above approach by studying several documented cases of fragmentation events and analyzing the calculated velocity perturbations by studying their frequency distributions, standard deviation and variance, and their relations to the radar cross-sections and plane change angles. New signs for characteristic features of the various types of breakups have been sought and the results of the study are then used to reclassify a few unknown categories of satellite breakups.

EQUATIONS

The changes in the three orthogonal components of velocity of a fragment Δv_r , Δv_θ and Δv_z (henceforth denoted by Δv_x) can be determined from the observed changes in the semi-major axis, eccentricity and inclination Δa , Δe and Δi from the following equations (Meirovitch, 1970):

$$\Delta a = \frac{2(1-e^2)^{\frac{1}{2}}}{n} \left[\frac{e \sin \theta}{1-e^2} \Delta v_r + \frac{a}{r} \Delta v_\theta \right] , \quad (1)$$

$$\Delta e = \frac{(1-e^2)^{\frac{1}{2}}}{na} \left[\sin \theta \Delta v_r + \frac{e}{ar} (1-e^2 - \frac{r^2}{a^2}) \Delta v_\theta \right] , \quad (2)$$

$$\text{and } \Delta i = \frac{r \cos(\omega+\theta)}{na^2(1-e^2)^{\frac{1}{2}}} \Delta v_x , \quad (3)$$

where a is the semi-major axis, e the eccentricity, r the radial distance, n the mean motion, ω the argument of perigee and θ the true anomaly at the point of fragmentation. Eliminating Δv_r and Δv_θ from Eqs.(1) and (2) and rewriting,

$$\Delta v_r = \frac{na^2(1-e^2)^{\frac{1}{2}}}{2er^2 \sin \theta} \left[2ae \Delta e - (1-e^2 - \frac{r^2}{a^2}) \Delta a \right] , \quad (4)$$

$$\Delta v_\theta = \frac{na(1-e^2)^{\frac{1}{2}}}{2r} \left[\Delta a - \frac{2ae}{1-e^2} \Delta e \right] , \quad (5)$$

$$\text{and } \Delta v_x = \frac{na^2(1-e^2)^{\frac{1}{2}}}{r \cos(\omega+\theta)} \Delta i . \quad (6)$$

The orbital elements of cataloged satellite fragmentation events are readily available from a technical report by Johnson, et al. (1986) in which the following quantities are cataloged whenever available: the inclination i , altitude of breakup h , altitude of perigee h_p , altitude of apogee h_a , true anomaly θ , the time period T , latitude λ and longitude ϕ . If r_0 is the radius of the earth, we have immediately:

$$a = \frac{r_a + r_p}{2} = \frac{2r_o + h_a + h_p}{2} , \quad (7)$$

$$e = \frac{r_a - r_p}{r_a + r_p} = \frac{h_a - h_p}{2r_o + h_a + h_p} , \quad (8)$$

$$\text{and} \quad r = r_o + h . \quad (9)$$

$$\text{Also,} \quad n = \frac{2\pi}{T} = \left(\frac{\mu}{a^3} \right)^{\frac{1}{2}} , \quad (10)$$

where μ , the product of the universal gravitational constant G and the mass of the earth M , is referred to as the gravitational parameter. The argument of latitude $u = \omega + \theta$ can be calculated as follows. Since u is the angle between the ascending node (λ_o, ϕ_o) and the event point (λ, ϕ) , we have (cf. Gellert, et al., 1977)

$$\cos u = \sin \lambda \sin \lambda_o + \cos \lambda \cos \lambda_o \cos(\phi - \phi_o) . \quad (11)$$

Now $\lambda_o = 0^\circ$ and ϕ_o can be read from the satellite map (Johnson, et al., 1986), whence

$$u = \cos^{-1} [\cos \lambda \cos(\phi - \phi_o)] . \quad (12)$$

The semi-major axis, eccentricity and inclination of the fragments are read from NORAD data files, from which Δa , Δe and Δi are calculated.

RESULTS

Altogether 23 major satellite fragmentation events belonging to the following categories were studied: collision induced breakups, e.g., Solwind P-78; low-intensity explosion induced breakups, e.g., Delta 2nd stage rocket explosions due to hypergolic fuel ignition; high-intensity explosion induced breakups, e.g., planned fragmentations of Cosmos satellites as part of alleged Soviet ASAT tests; and unknown categories. These events contributed to nearly 80% of all documented debris from satellite fragmentation events. Double and multiple events were not considered in this study.

An inspection of Eq.(4) reveals that the values of Δv_r become exceedingly high in the following cases. First, if the fragmentation took place near the apogee (e.g., NOAA-3, NOAA-4 and Transit 4A rockets) or near perigee (e.g., Cosmos 252 and Cosmos 375 satellites), then the small denominator in Eq.(4) yields unusually high values for Δv_r . Taking natural logarithms and differentiating both sides of Eq.(4), we get

$$\frac{d(\Delta v_r)}{\Delta v_r} = \frac{dn}{n} + \frac{2}{a} \frac{da}{a} + \frac{\frac{1}{2} d(1-e^2)}{1-e^2} + \frac{df}{f} - \frac{de}{e} - \frac{2}{r} \frac{dr}{r} - \frac{d(\sin\theta)}{\sin\theta} ,$$

$$\text{where } f(a,e,\Delta a,\Delta e) = 2ae \Delta e - (1-e^2 - \frac{r^2}{a^2}) \Delta a .$$

Simplifying and rearranging,

$$\frac{d(\Delta v_r)}{\Delta v_r} = \frac{dn}{n} + \frac{2}{a} \frac{da}{a} - \frac{de}{e(1-e^2)} + \frac{df}{f} - \frac{2}{r} \frac{dr}{r} - \cot\theta d\theta . \quad (13)$$

Evidently, the percentage error in Δv_r due to the last term in Eq.(13) alone is infinite at apogee ($\theta = 180^\circ$) or perigee ($\theta = 0^\circ$). Even with an accuracy of $d\theta = 1^\circ$, the percentage errors owing to the last term at 1° , 2° and 3° on either side of apogee and perigee are 100%, 50% and 33% respectively. Secondly, for nearly circular orbits having eccentricities of 0.002 or less (e.g., NOAA-3, NOAA-4, NOAA-5 Landsat 3 and OPS 7613

rockets, Cosmos 1375 and Solwind satellites and Spot 1 Ariane 3rd stage rocket), the second term in Eq.(4) again dictates high values of the same sign for Δv_r . Equation (6) also indicates that Δv_x can have abnormally high values when the argument of latitude is close to 90° or 270° . However, we did not encounter an actual case like that in our examples. The values of Δv_θ , on the other hand, were always realistic.

Thus, to sum up, the calculated values of Δv_r were frequently unreliable, whereas the values of Δv_θ and Δv_x were mostly reliable. Hence the rest of this study was focussed on Δv_θ and Δv_x and not on Δv_r . Further, since the large values of Δv_r necessarily translate into large values of Δv , the net velocity change, its role in this study was also minimized.

Figure 1 is an illustrative example of the frequency distributions of the velocity perturbations. The fragments belonged to Solwind which was intentionally destroyed through hypervelocity impact as part of an alleged US ASAT Test (Kling, 1986). The distributions of Δv_θ and Δv_x were closer to Gaussian ones than that of Δv_r . There were slightly more negative values in Δv_θ and slightly more positive values in Δv_x but the Δv_r 's were mostly negative. This is almost certainly due to the nearly circular orbit of Solwind prior to the breakup ($e = 0.0022$) as discussed earlier. The distribution of Δv is more or less exponential as expected.

The magnitude of Δv has been used as one of the prime criteria in distinguishing between explosion and collision induced breakups by McKnight (Culp, 1986). According to earth-based experiments, the larger fragments will acquire much larger velocity perturbations in an explosion than in a collision (Bess, 1975). Our calculations give the lowest values to Δv 's for Cosmos 839 and Cosmos 1375, which would almost certainly place them in the collision category, in general agreement with the analysis of McKnight (Culp, 1986). The Cosmos 1275 and Solwind P-78 fragments had significantly higher Δv 's but they were still considerably smaller than those of explosive fragments. It may be noted that Cosmos 1275 is classified in the collision category by McKnight (Culp, 1986),

SOLWIND SEP 13, 1985

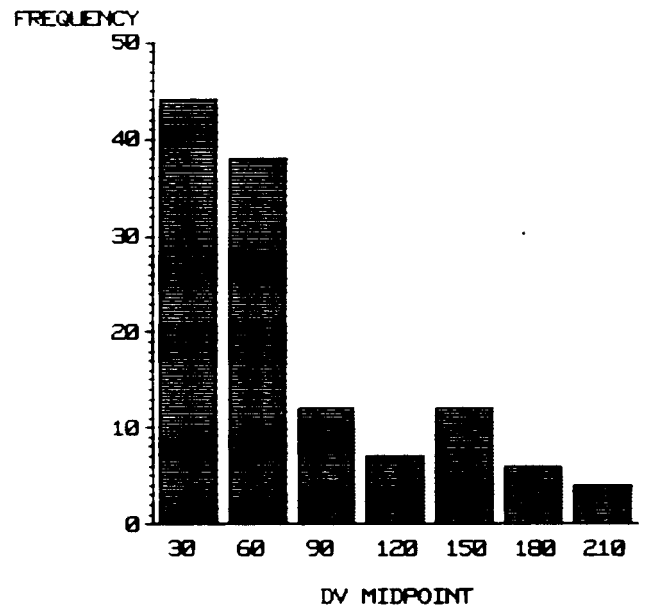
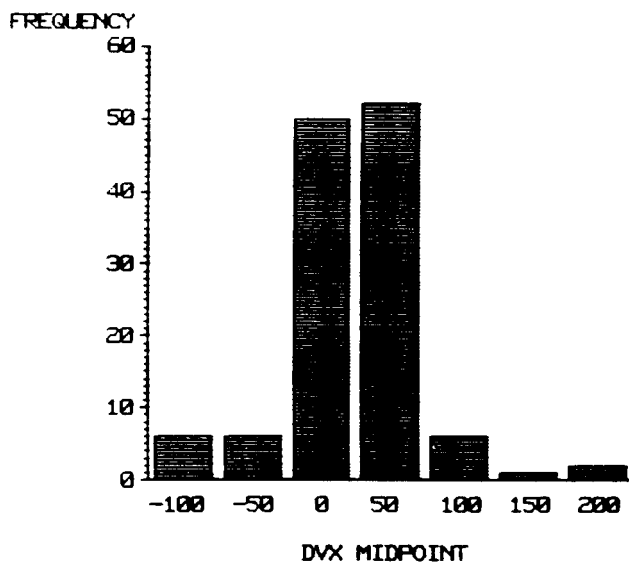
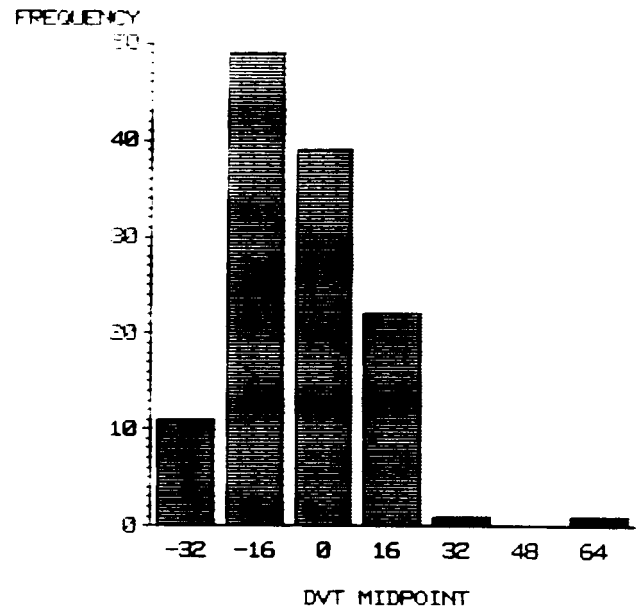
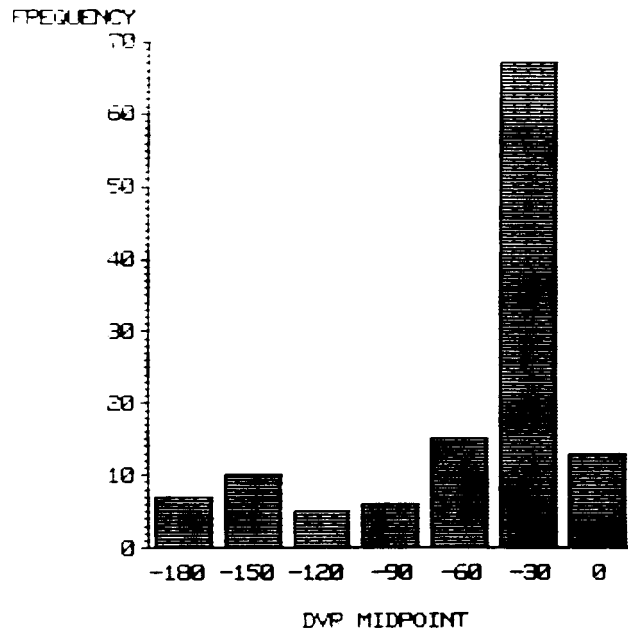


Fig. 1. Frequency distributions of Δv_r , Δv_θ , Δv_x and Δv of fragments of Solwind P-78. The velocities are in units of m/s.

but the analysis of Badhwar, et al. (1987) places a much smaller probability for that likelihood. However, one cannot put too much emphasis on the magnitudes of the velocity perturbations bearing in mind the uncertainties in Δv_r and consequently those in Δv .

Figure 2 is a two-dimensional plot of the velocity perturbations of Solwind fragments in the θ - x plane. The relative magnitudes of the rcs values of the fragments are also indicated in the diagram. In the case of a collision with a small object, one would expect the smaller fragments to be dispersed more than the larger ones (Bess, 1975), but that is not very evident from the diagram. One must recall, however, that Solwind was made to collide with an object of comparable mass (Kling, 1986). Moreover, a collision can range from a head-on collision to a glancing one and each can have its own characteristics.

Figure 3 is a three-dimensional plot of the orthogonal components of the velocity perturbations of Solwind fragments. The relative magnitudes of the rcs values are, once again indicated in the diagram. There seems to be the appearance of a main cluster of fragments together with a more dispersed secondary one. But in view of the uncertainties in Δv_r , this feature cannot be taken seriously.

Figure 4 is a plot of the frequency distributions of velocity perturbations of the Solwind fragments in the θ - x plane. A close scrutiny reveals the appearance of a relatively small scatter of the fragments. Also conspicuous are two well-defined peaks, which was a unique feature among all the fragmentation cases studied. Whether the two peaks belonged to the interceptor and the target parents is impossible to ascertain at present.

Figure 5 is a similar plot for the fragments of NOAA-5 second stage rocket, which is one of the several cases of low-intensity explosion involving a Delta second stage rocket. Here, the scatter of the fragments is relatively large. Also there is only one main peak in the frequency plot.

SOLWIND

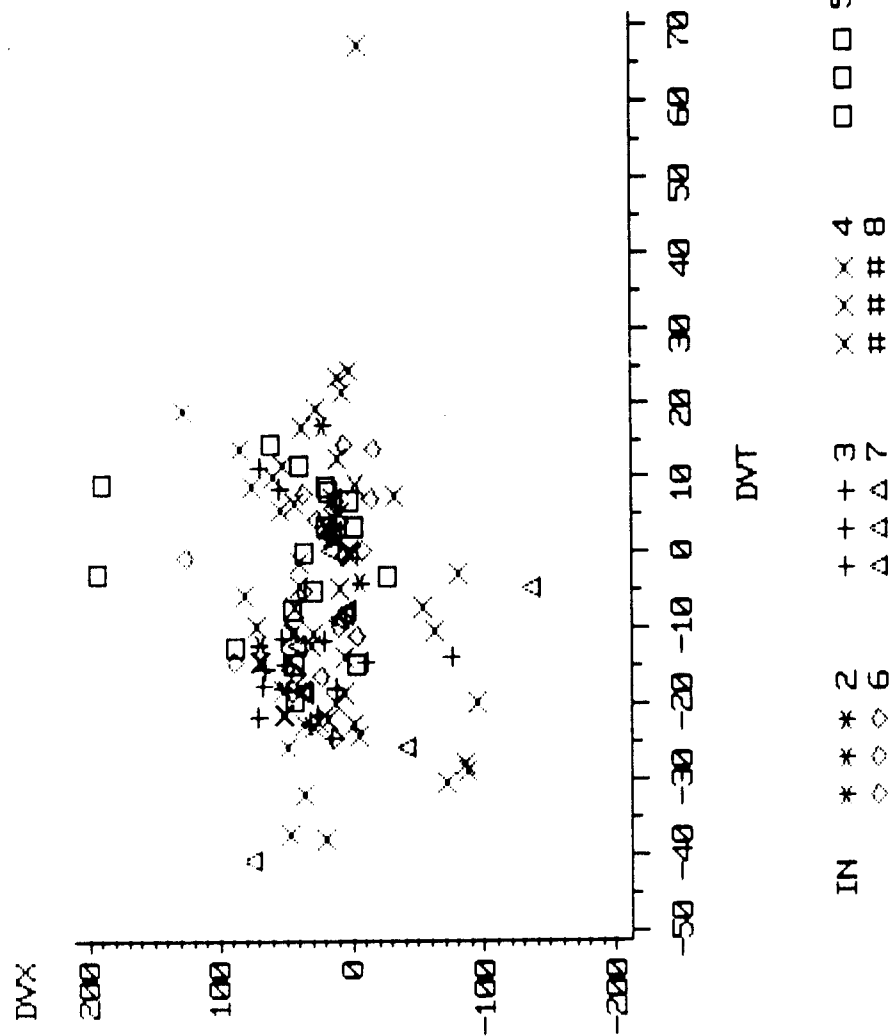


Fig. 2. Velocity perturbations plot of Solwind fragments in the $\theta - x$ plane. Also shown in the figure are the rcs values of the fragments in increasing numerical order.

SOLWIND

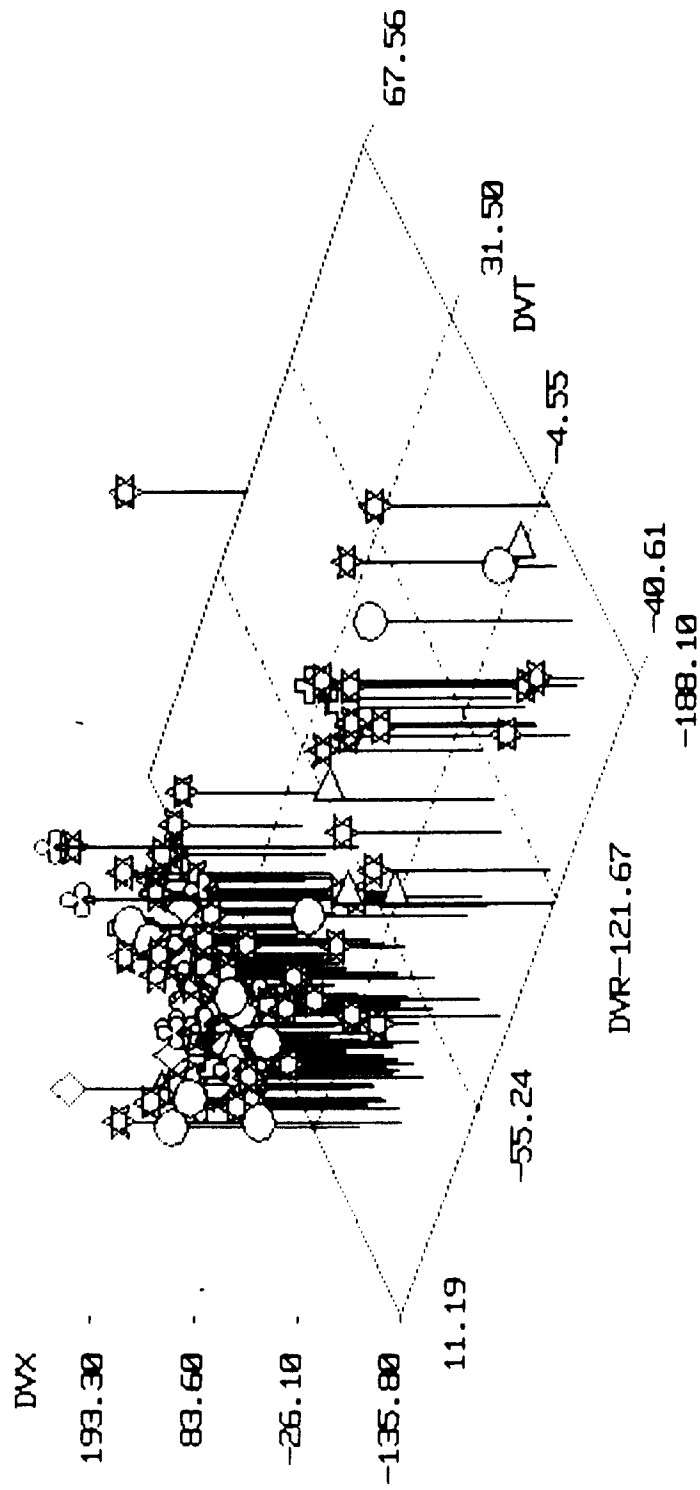


Fig. 3. Three-dimensional plot of velocity perturbations of Solwind fragments. The shapes indicate the magnitudes of RCS in the following increasing order: cylinder, cross, balloon, star, club, diamond, flag, heart, pyramid and square.

SOLWIND FEB 77

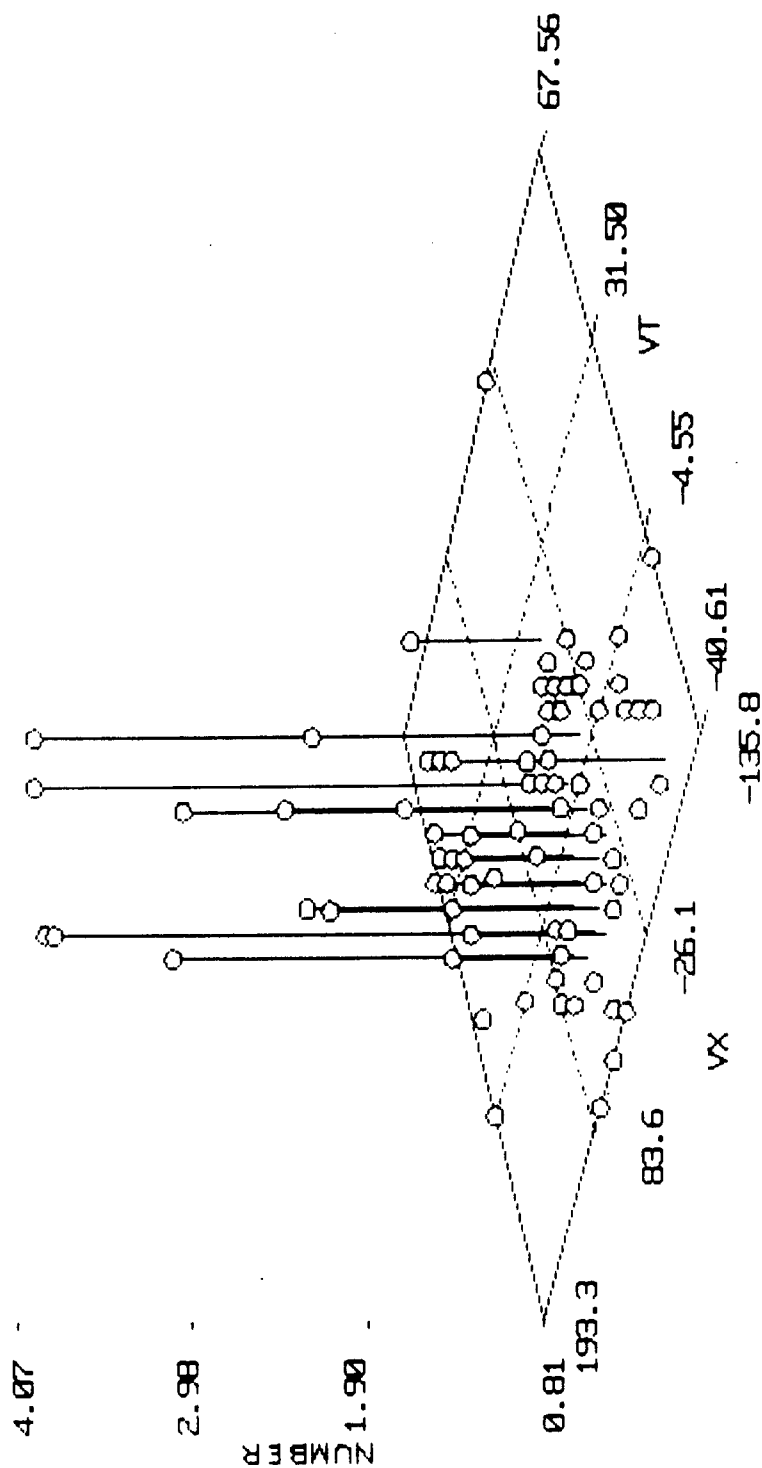


Fig. 4. Frequency distribution of velocity perturbations of the Solwind fragments in the θ -x plane. The velocities are in the units of m/s.

BREAKUP OF NOAA 5

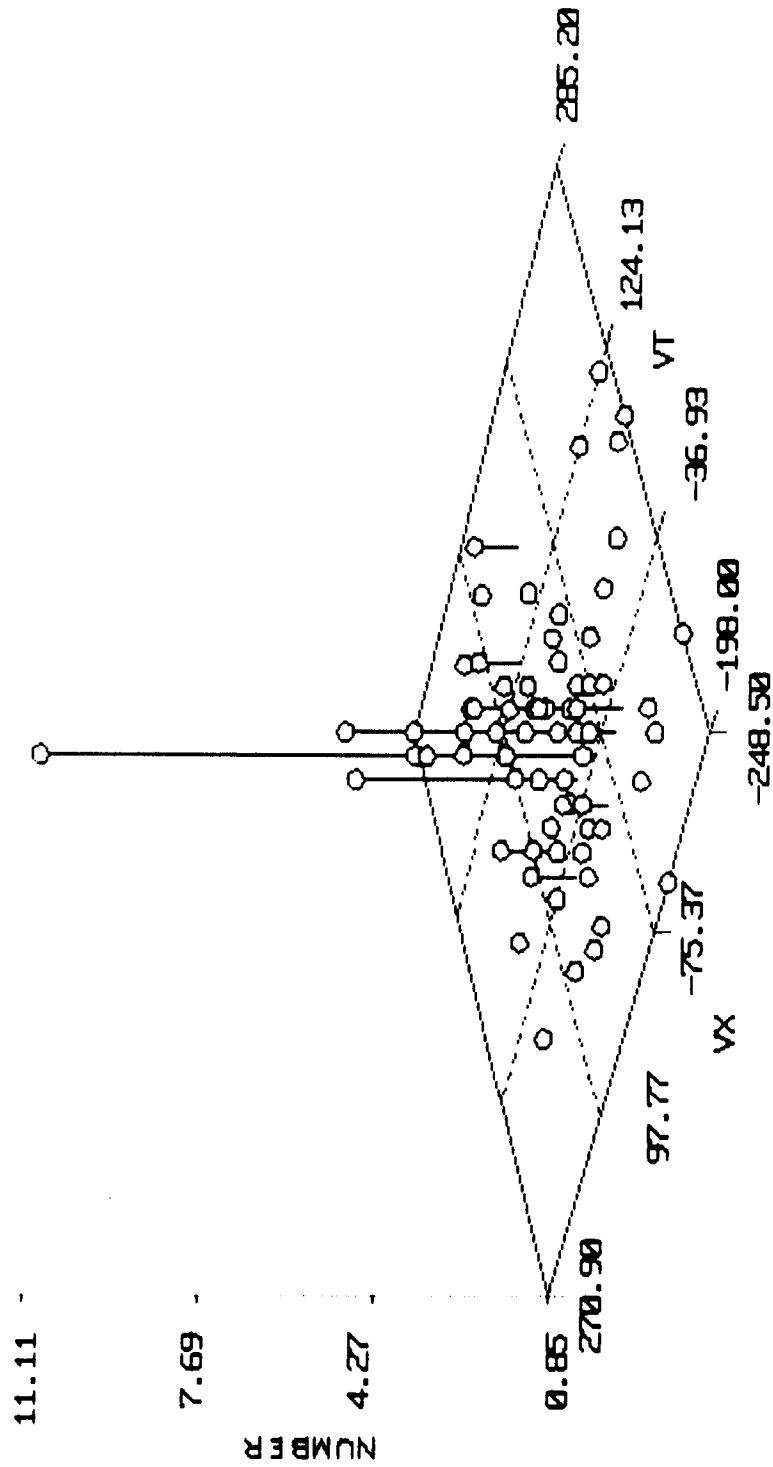


Fig. 5. Frequency distribution of velocity perturbations of NOAA-5 fragments in the θ -x plane. The velocities are in the units of m/s.

Calculated variances of the velocity perturbations betray a most important finding of this study: the collision induced breakups have the least variances in Δv_{θ} and Δv_x and the low-intensity explosion induced breakups have the highest variances in Δv_{θ} and Δv_x whereas the high-intensity explosion induced breakups generally have variances intermediate between the two extreme classes. This is, of course, not inconsistent with the mechanisms of the breakups. A low-intensity explosion, like a pressure tank burst from deflagration in a Delta or Thor-Agena rocket produces fragments with a large velocity distribution whereas a high-intensity explosion like deliberate detonations of Cosmos series satellites produces fragments of more or less uniform velocity, i.e., with small velocity distribution (Benz, et al., 1987).

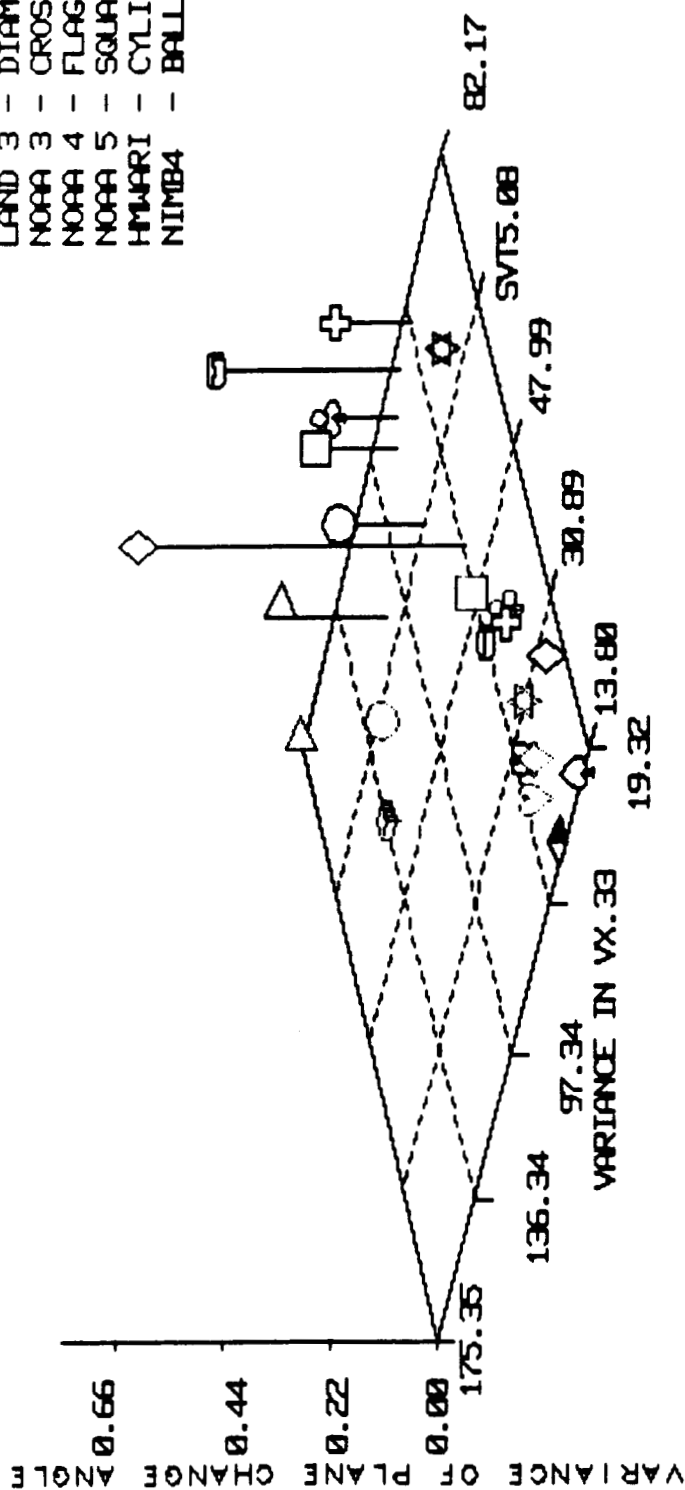
The above finding provides us with a scheme to separate the three types of satellite fragmentations: collision induced, low-intensity explosion induced and high-intensity explosion induced breakups. Figure 6 is a plot of the variances in Δv_{θ} and Δv_x with the variance of the plane change angle as the vertical axis. The plane change angles were taken from the study of Badhwar, et al. (1987). The positions of the satellites in the 3-space of Fig.6 clearly separate themselves out according to the following scheme:

Collision induced breakups low variances in Δv_{θ} , Δv_x and pca
 High-intensity explosions ... Intermediate variances in the above
 Low-intensity explosions High variances in the above

The three satellites with the lowest variances were Cosmos 1375, Solwind P-78 and Cosmos 839, thus reaffirming the assertion that Cosmos 1375 and Cosmos 839 were target satellites in Soviet ASAT tests. Cosmos 1275, contrary to McKnight's analysis (Culp, 1986), places itself in the high-intensity explosion category as does Cosmos 61-63. Nimbus 4 and Transit 4A rockets have all the signs of belonging to the low-intensity explosion category.

It must be pointed out that the present study, like the Gabbard diagram

LAND 1 - CLUB
 LAND 3 - DIAM
 NOAA 3 - CROS
 NOAA 4 - FLAG
 NOAA 5 - SQUA
 HMARI - CYLI
 NIMB4 - BALL



K61-3 : STAR 07613 : HEART TRANS : CYL K1275: CROSS
 K1375 : SPAD K839 : DIAM SOLWIND : PYRA
 1252 : BALL 1970 : DIAM 1886 : STAP 1397 : CUBE 1375 : HEART
 1374 : CLUB K1274 : SQUA K249 : FLAG
 UNKNOWN EXPLOSION COLLISION DELTA/AGENA

Fig. 6. Three-dimensional plot of variances of Δv_θ , Δv_x and pca .

studies of Culp and McKnight (Culp, 1986), suffers from the "ageing" of the fragment data. To obtain the best results, one needs the orbital elements of the parent just prior to the breakup as well as those of the fragments right after it. Unfortunately, this is seldom realized unless we can anticipate a breakup beforehand and make the necessary observations. In our examples, oftentimes the data were years old and several fragments had already decayed. The "youngest" data, on the other hand, often contained the fewest number of pieces. A judicious compromise always calls for a subjective decision of the user.

Lastly, we should seek alternative expressions for the velocity perturbations which do not pose such problems as encountered in this study. For example, in the case of nearly circular orbits, the radial component of the velocity perturbation may be approximated by the normal component, the expression for which is given by Ehricke (1962):

$$v_n = - \frac{a v \Delta e}{r \sin \theta} . \quad (14)$$

Here, v is the tangential velocity of the parent at the point of fragmentation.

CONCLUSIONS

- (1) An analysis of calculating velocity perturbations of fragments of a disintegrated satellite indicates that whereas the radial components frequently had abnormally high values, the components in the other two orthogonal directions had mostly acceptable values.
- (2) The calculated variances in Δv_{θ} and Δv_x indicate that the collision induced breakups had the least variances, the high-intensity explosion induced breakups had higher variance while the low-intensity explosion induced breakups had the highest variances.
- (3) A three-dimensional plot of the variances in Δv_{θ} , Δv_x and pca showed a clear separation in the three types of satellite breakups which can therefore be used to reclassify breakups of unknown causes.
- (4) Cosmos 1375 and Cosmos 839 are thus reclassified as collision induced breakups; Cosmos 1275 and Cosmos 61-63 are reclassified into the high-intensity explosion category while Nimbus 4 and Transit 4A rockets are reclassified into the low-intensity explosion category.
- (5) Other quantities from the satellite fragment data, such as angular momentum change, energy change, decay rates, etc. may also provide valuable information regarding the nature of satellite breakups and they could be undertaken as logical extension of this study.

REFERENCES

- G. D. Badhwar, A. E. Potter, P. Anz-Meador and R. C. Reynolds, Preprint, 1987.
- F. J. Benz, C. V. Bishop and M. B. Beck, Preprint, 1987.
- T. D. Bess, NASA Tech. Note D-8108, Langley Research Center, 1975.
- V. A. Chobotov, J. Spacecraft & Rockets, 20, 484, 1983.
- R. D. Culp, Teledyne Brown Engg. Contract SC 7460, 1986.
- K. A. Ehricke, Space Flight. II. Dynamics, Van Nostrand Co., Inc., Princeton, 1962, p.352.
- W. Gellert, H. Kustner, M. Hellwich and H. Kastner, The VNR Encyclopedia of Mathematics, Van Nostrand Reinhold Co., New York, 1977, p.213.
- N. L. Johnson, Communications with R. D. Culp, 1985.
- N. L. Johnson, J. R. Gabbard, R. L. Kling, Jr. and T. W. Jones, Teledyne Brown Engg. Tech. Rept. No. CS86-USASDC-0001, 1986.
- D. J. Kessler and B. G. Cour-Palais, J. Geophys. Res., 83, 2637, 1978.
- R. Kling, Teledyne Brown Engg. Rept. CS86-LKD-001, 1986.
- L. Meirovitch, Methods of Analytical Dynamics, McGraw-Hill Book Co., New York, 1970, p.456.
- NORAD Space Surveillance Center (NSSC) Satellite Catalog, 1985.
- R. C. Reynolds, Personal Communication, 1987.
- L. Sehnal, COSPAR Meeting Presentation, 1984.
- L. G. Taff, D. E. Beatty, A. J. Yakutis and P. M. S. Randall, COSPAR Meeting Presentation, 1984.